Supplement

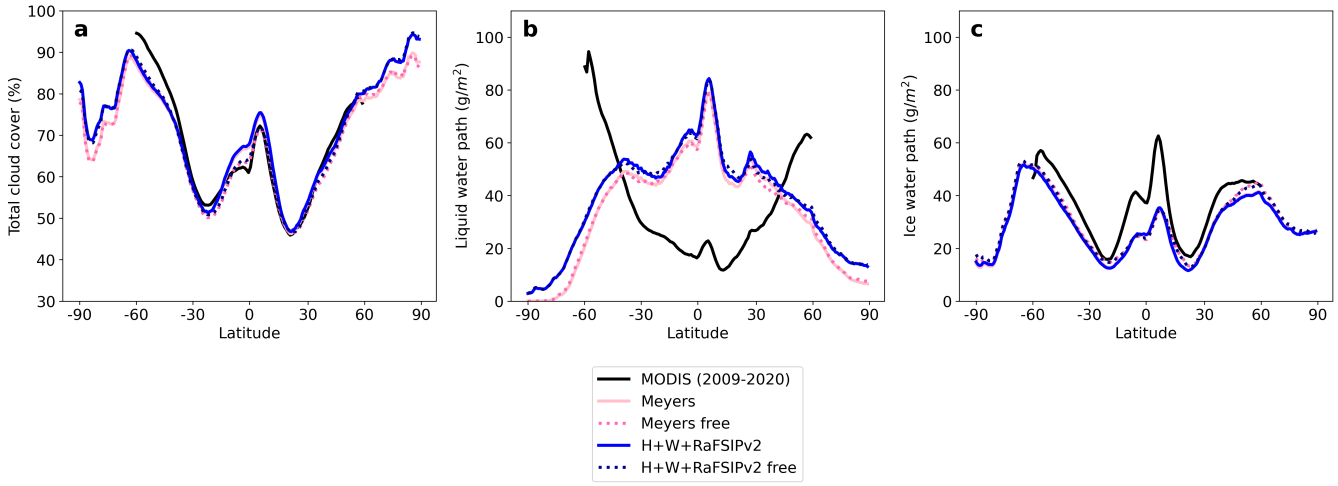

Figure S1. Zonal mean of the total cloud cover, LWP, and IWP for the period 2009-2020, following Meyers et al. (1992) and the aerosol-sensitive ice nucleation parameterization by Harrison et al. (2019) and Wilson et al. (2015) alongside the RaFSIPv2 parameterization in nudged and free (i.e., without nudging) setups. Results are compared with MODIS observations.

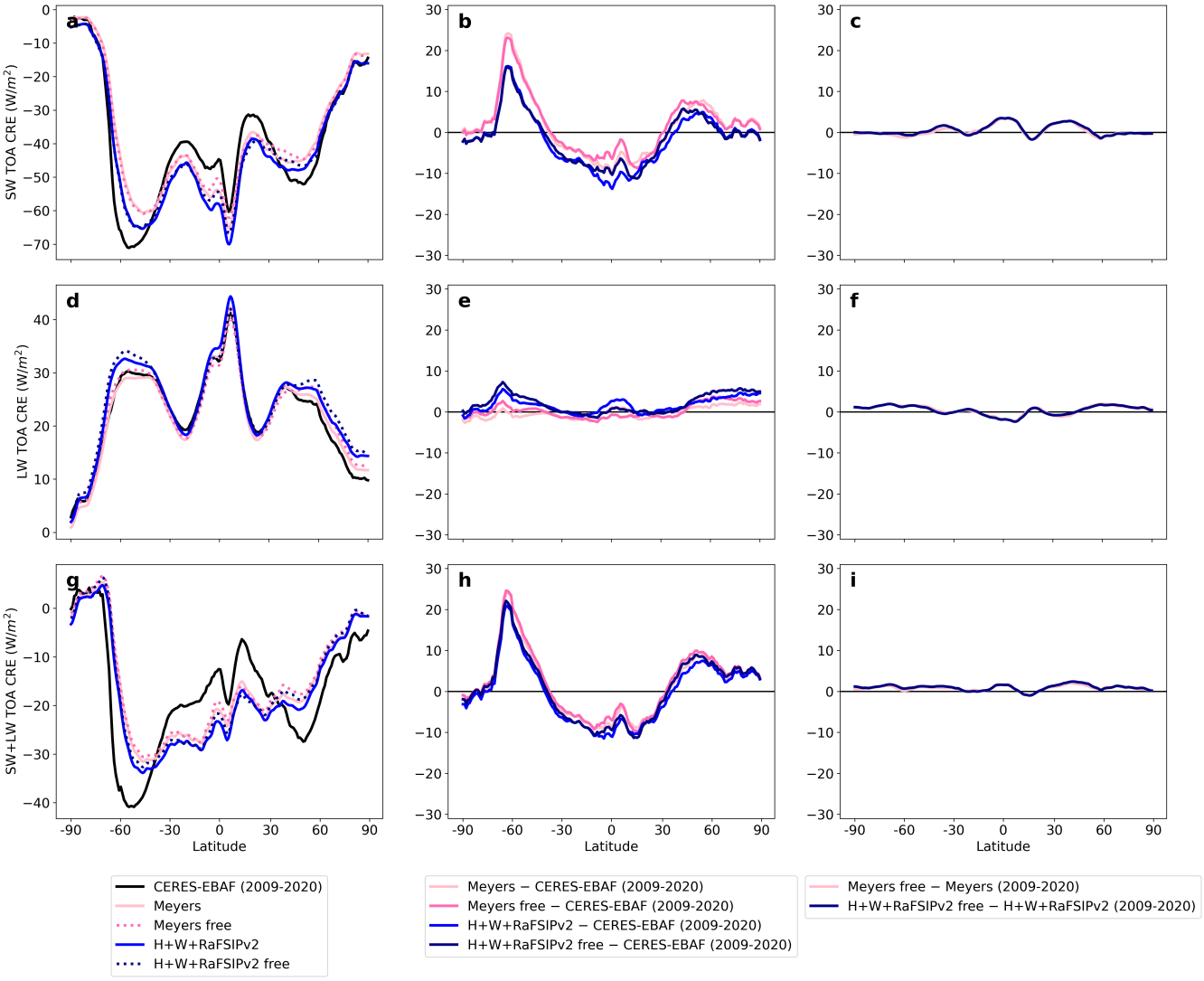

Figure S2. Left column: Zonally averaged, climatological (2009–2020) mean TOA SW, LW and net (SW+LW) CRE, following Meyers et al. (1992) and the aerosol-sensitive ice nucleation parameterization of Harrison et al. (2019) and Wilson et al. (2015) in combination with the RaFSIPv2 parameterization in their nudged and free setups. Middle column: Differences between the simulations and the observations of CERES-EBAF. Right column: Radiative flux differences between the free and nudged simulations. Note that all these figures have to be read taking into account that the model has only been tuned for the ice nucleation parameterization that follows Meyers et al. (1992) (refer to Sect. 3 in van Noije et al. (2021) for more details).

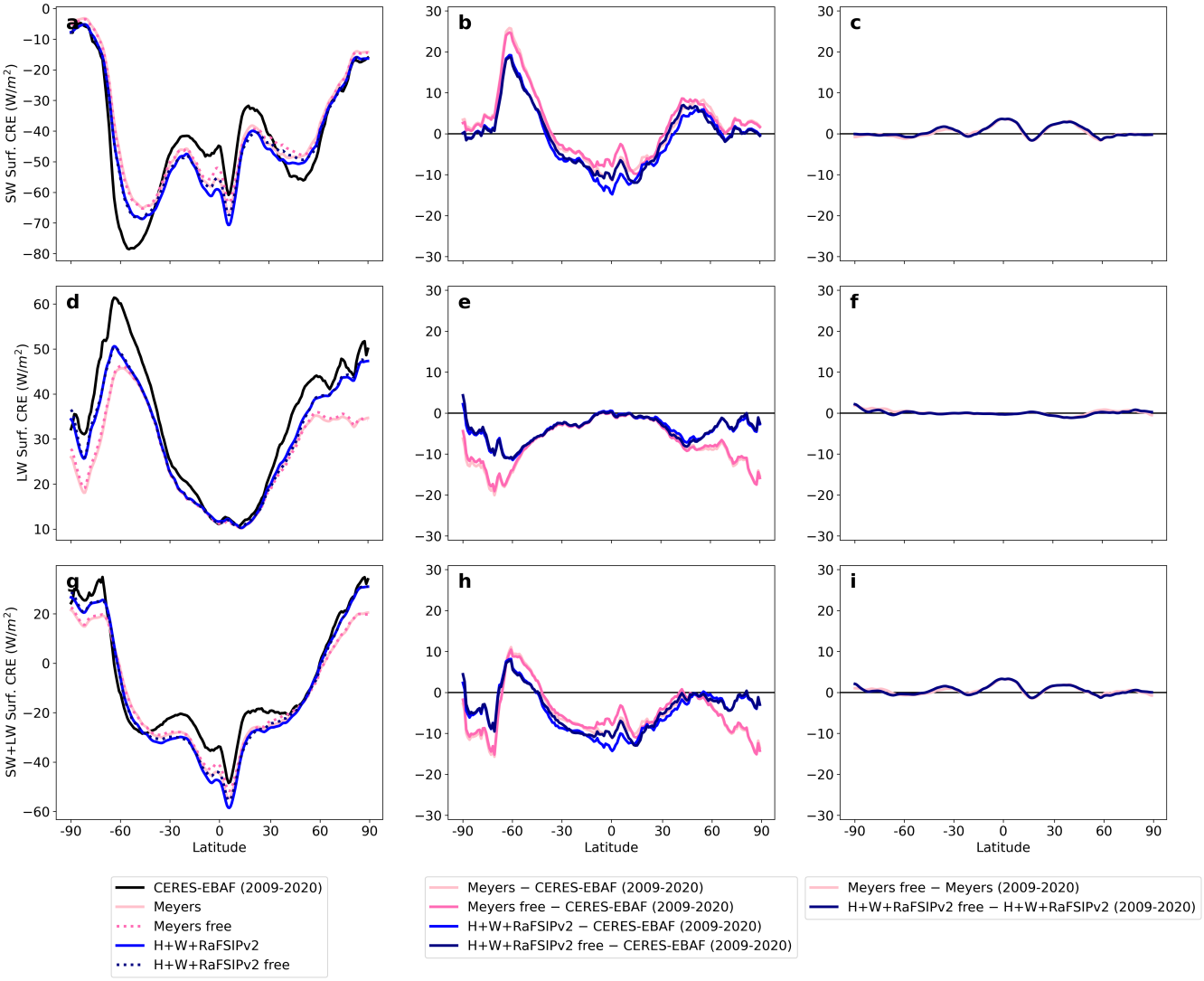

Figure S3. Left column: Zonally averaged, climatological (2009–2020) mean Surface SW, LW and net (SW+LW) CRE, following Meyers et al. (1992) and the aerosol-sensitive ice nucleation parameterization of Harrison et al. (2019) and Wilson et al. (2015) in combination with the RaFSIPv2 parameterization in their nudged and free setups. Middle column: Differences between the simulations and the observations of CERES-EBAF. Right column: Radiative flux differences between the free and nudged simulations. Note that all these figures have to be read taking into account that the model has only been tuned for the ice nucleation parameterization that follows Meyers et al. (1992) (refer to Sect. 3 in van Noije et al. (2021) for more details).

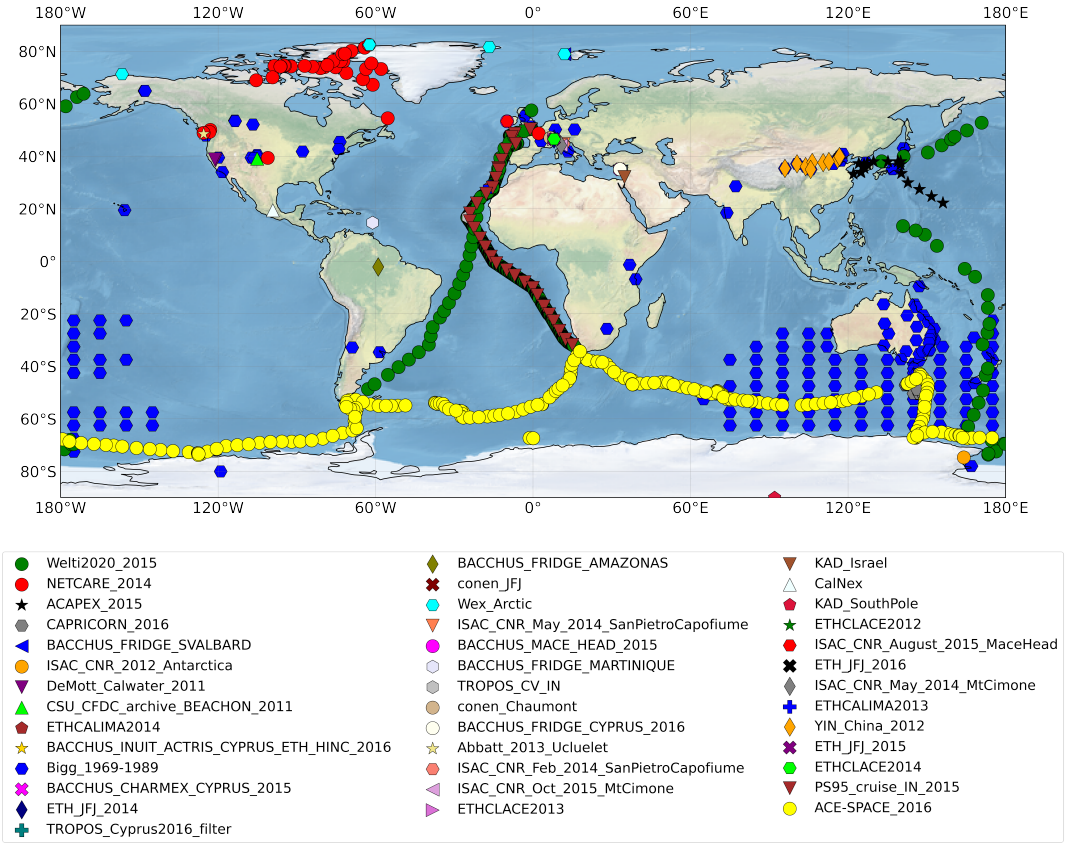

Figure S4. Locations of the data used in the INP evaluation presented in Fig. 1.

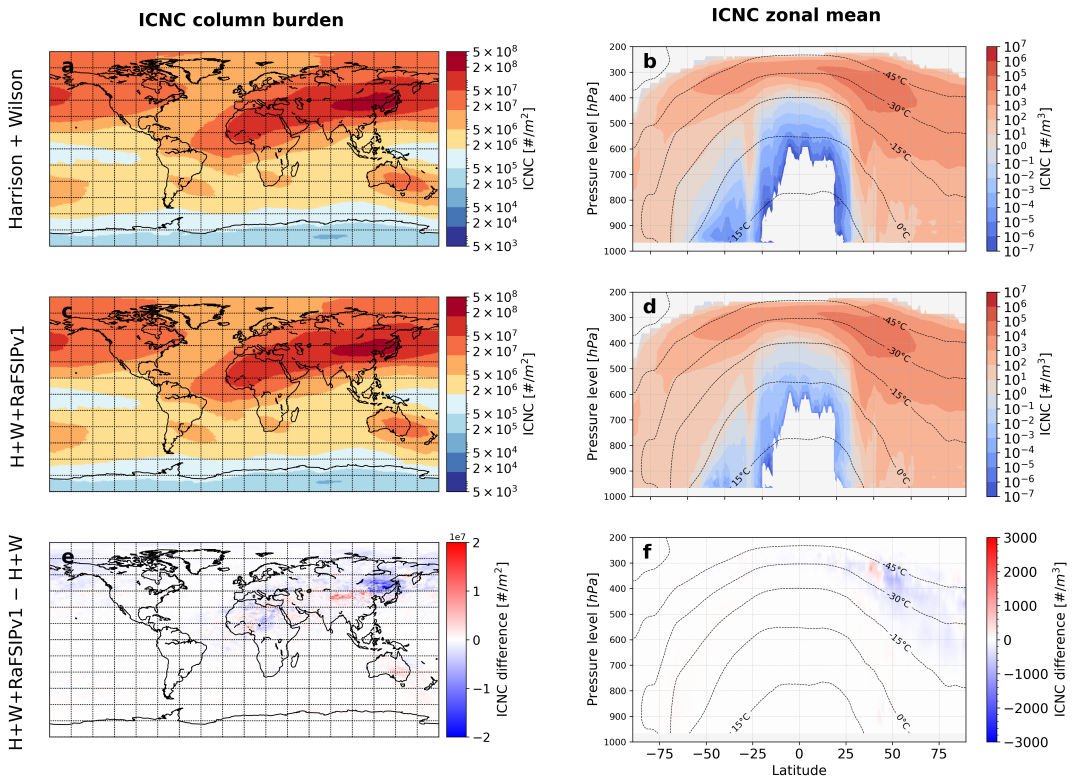

Figure S5. Left panels show the multi-annual global distribution of column MPCs ICNC load when using (a) the Harrison et al. (2019) parameterization for K-feldspar and quartz minerals in combination with the Wilson et al. (2015) for marine organic aerosols parameterizations, (b) the Harrison et al. (2019) in combination with the Wilson et al. (2015) and RaFSIPv1 (Georgakaki and Nenes, 2024), and (c) the difference between (b) and (a). The right panels show the corresponding multi-annual zonal means of the MPCs ICNC concentration (isotherms represent all-sky grid-cell atmospheric temperature averages, not in-cloud means).

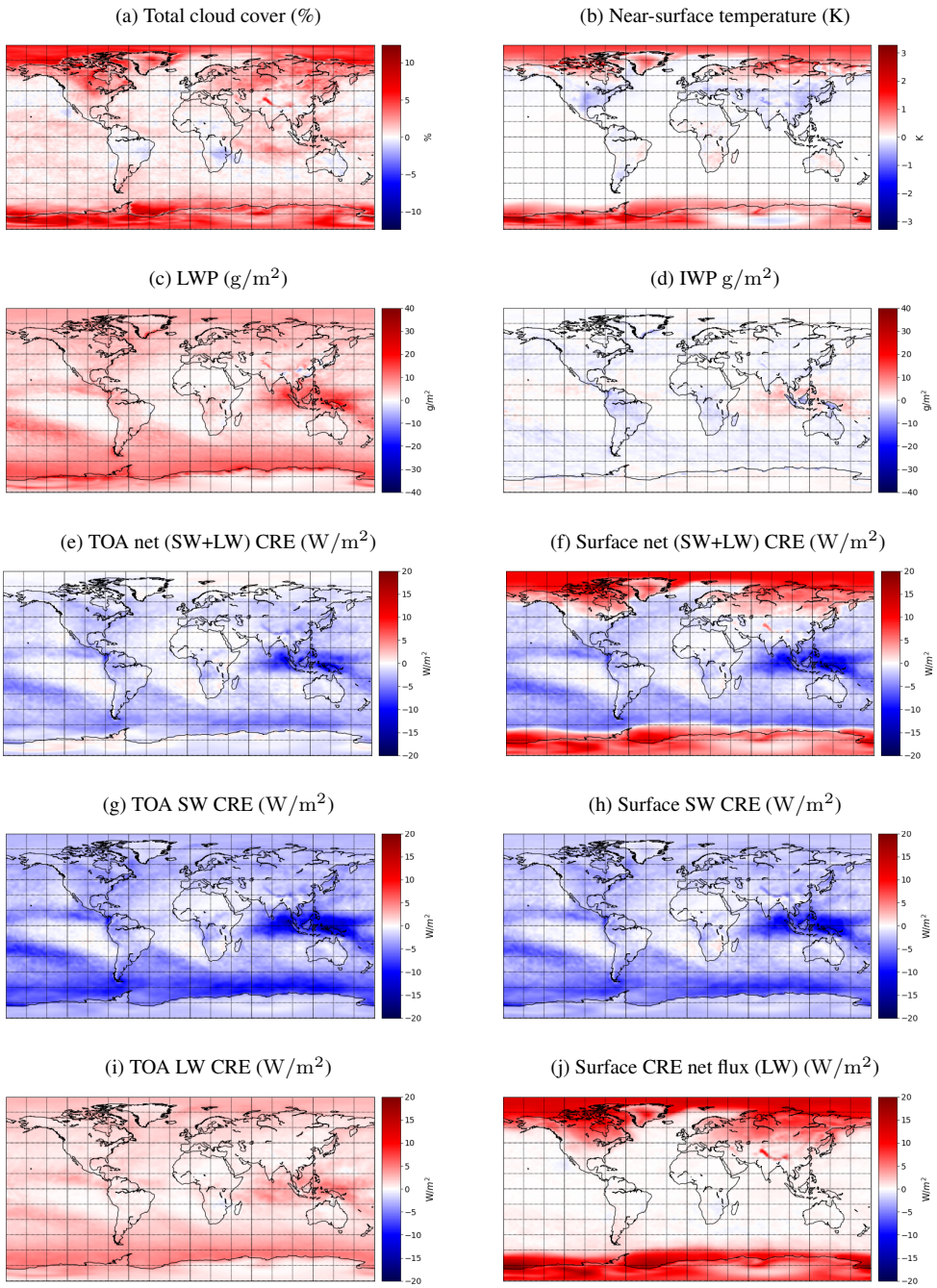

Figure S6. Multi-year (2009-2020) global mean differences between the nudged simulation done with the aerosol-sensitive ice nucleation parameterization following Harrison et al. (2019) + Wilson et al. (2015) + RaFSIPv2 and the one using Meyers et al. (1992) parameterization, for the variables: cloud cover, LWC, IWC, near-surface temperature, TOA SW, LW and net (SW+LW) CRE, and surface SW, LW and net (SW+LW) CRE.

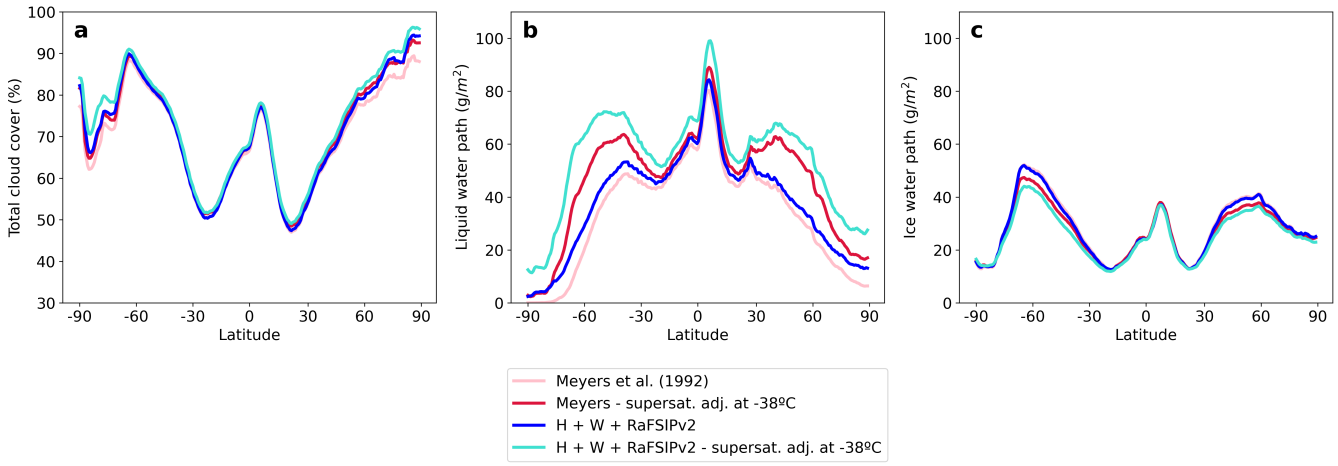

Figure S7. 1-year (2018) zonal means of total cloud cover, LWC and IWC, following Meyers et al. (1992) and the aerosol-sensitive ice nucleation parameterization Harrison et al. (2019) and Wilson et al. (2015) in combination with the RaFSIPv2 parameterization, compared with results from the corresponding simulations but with the supersaturation adjustments taking place at -38 °C.